



**HAL**  
open science

## Refinement of digital image correlation technique to investigate the fracture behaviour of refractory materials

Younès Belrhiti, Octavian Pop, A. Germaneau, Pascal Doumalin, J.C. Dupré,  
Marc Huger, Thierry Chotard

### ► To cite this version:

Younès Belrhiti, Octavian Pop, A. Germaneau, Pascal Doumalin, J.C. Dupré, et al.. Refinement of digital image correlation technique to investigate the fracture behaviour of refractory materials. IOP Conference Series: Materials Science and Engineering, 2016, 119, pp.012010. 10.1088/1757-899X/119/1/012010. hal-01877741

**HAL Id: hal-01877741**

**<https://unilim.hal.science/hal-01877741>**

Submitted on 20 Sep 2018

**HAL** is a multi-disciplinary open access archive for the deposit and dissemination of scientific research documents, whether they are published or not. The documents may come from teaching and research institutions in France or abroad, or from public or private research centers.

L'archive ouverte pluridisciplinaire **HAL**, est destinée au dépôt et à la diffusion de documents scientifiques de niveau recherche, publiés ou non, émanant des établissements d'enseignement et de recherche français ou étrangers, des laboratoires publics ou privés.

PAPER • OPEN ACCESS

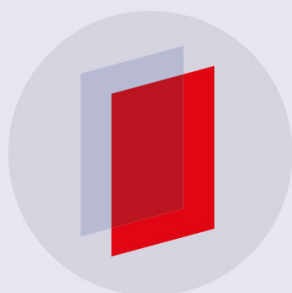
## Refinement of digital image correlation technique to investigate the fracture behaviour of refractory materials

To cite this article: Y. Belrhiti *et al* 2016 *IOP Conf. Ser.: Mater. Sci. Eng.* **119** 012010

View the [article online](#) for updates and enhancements.

### Related content

- [Strain controlled cyclic tests on miniaturized specimens](#)  
R Procházka and J Džugan
- [Brazilian disc experiments on a cold spray material](#)  
C H Braithwaite, B Aydelotte and A P Jardine
- [Combined Experimental and Numerical Study on Fracture Behaviour of Low-Density Foamed Concrete](#)  
M Kozowski and M Kadela



**IOP | ebooks™**

Bringing you innovative digital publishing with leading voices to create your essential collection of books in STEM research.

Start exploring the collection - download the first chapter of every title for free.

# Refinement of digital image correlation technique to investigate the fracture behaviour of refractory materials

Y.Belrhiti<sup>1</sup>, O. Pop<sup>2</sup>, A.Germaneau<sup>3</sup>, P.Doumalin<sup>3</sup>, J.C.Dupré<sup>3</sup>, M.Huger<sup>1</sup>,  
T.Chotard<sup>1</sup>

<sup>1</sup> Science des Procédés Céramiques et Traitements de Surface (SPCTS UMR CNRS 7315), CEC, 12 rue Atlantis, 87068 Limoges Cedex, France

<sup>2</sup> Groupe d'Etude des Matériaux Hétérogènes (GEMH), Université de Limoges, 12 rue Atlantis, 87068 Limoges Cedex, France

<sup>3</sup> Institut Pprime, CNRS, Université de Poitiers, 11 Boulevard Marie et Pierre Curie, 86962 Futuroscope Chasseneuil Cedex, France

E-mail: pascal.doumalin@univ-poitiers.fr

**Abstract.** Refractory materials exhibit a heterogeneous microstructure consisting in coarse aggregates surrounded by fine grains that form an aggregate/matrix composite. This heterogeneous microstructure often leads to a complex mechanical behaviour during loading. This paper is devoted to the study, thanks to an optical method, Digital Image Correlation (DIC), of the fracture behaviour of two industrial refractory materials in relation with their microstructure resulting from both the chosen constituents and the sintering process. The aim is here, specifically, to highlight and to characterize the evolution of kinematic fields (displacement and strain) observed at the surface of sample during a wedge splitting test typically used to quantify the work of fracture. DIC is indeed a helpful and effective tool, in the topic of experimental mechanics, for the measurement of deformation in a planar sample surface. This non-contact optical method directly provides full-field displacements by comparing the digital images of the sample surface obtained before and during loading. In the present study, DIC has been improved to take into account the occurrence of cracks and performed so as to better identify the early stage of the cracking behaviour. The material transformation, usually assumed homogeneous inside each DIC subset, is thus more complex and a discontinuity of displacement should be taken into account. Then each subset which crosses a crack can be cut in two parts with different kinematics. By this way, it is possible to automatically find the fracture paths and follow the crack geometries (length, opening).

## 1. Introduction

Refractories, widely used in many industrial areas such as steel, cement, lime, non-ferrous metals and glass processing, are known for their ability to be used at very high temperature and to resist, in the same time, to significant levels of mechanical stress and strain. In addition, their ability to sustain thermal shocks is also, in many cases, of prime importance to avoid premature failure. This property of thermal shock resistance is known to be closely related to the crack growth behaviour of these materials ([1]-[3]). In this aim to promote crack growth resistance, an initial network of microcracks can be voluntary introduced within the microstructure which moves the mechanical behaviour, from a classical pure elastic to a material with pronounced R-curve behaviour, thus enhancing work of



fracture as well as strain to rupture. The tensile mechanical behaviour (Figure 1) is then typically characterized by a rather low stress-to-rupture and an important compliance (flexibility) of the material.

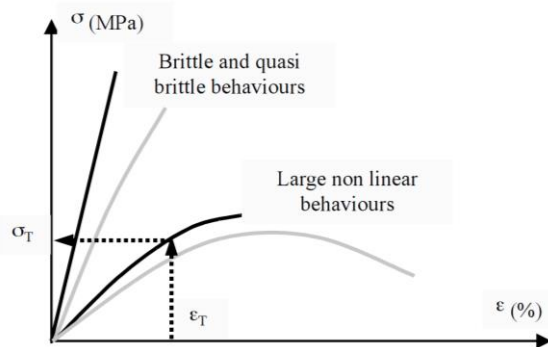


**Figure 1:** Typical stress/strain behaviours observed in tension on refractory materials [3]

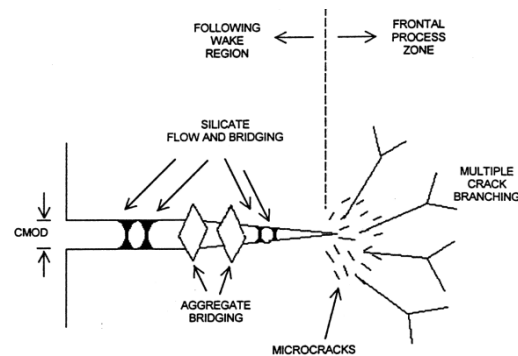


**Figure 2:** Schematic representation of the crack propagation zone for refractories [4]

During macrocrack opening, due to the initial network of microcracks intentionally introduced within the microstructure of the material, different complex inelastic phenomena will occur and consume a large amount of energy which will slow down the macrocrack propagation, leading to an increase in work of fracture [4]. The crack region can be divided to two areas: the frontal process zone and the following wake region as represented in Figure 2. The frontal process zone is localized ahead of the main crack and corresponds mainly to micro-cracking. It may lead to large crack branching phenomena depending on the initial microstructure. Thus, the size of this frontal process region depends on the type of refractory. The following wake region is located behind the crack front and across the fracture surface. The most important mechanisms are here the bridging across the created crack surfaces and the frictional effects due to the pull-out of the aggregates between the two sides of the passing crack.

The aim of the present paper is specifically to illustrate those different mechanisms by their direct visualisation at the surface of sample with the help of specific numerical treatments of images recorded during mechanical test. Non-contact optical methods are commonly used as for example Digital Image Correlation technique (DIC). This technique has been developed since several years to study 2D surface motions and it is a powerful method to study the behaviour of materials [5]-[8]. DIC is based on the analysis of successive images of the surface of the studied specimen during a mechanical test. At each state of load, a displacement field is calculated by measuring the degree of similarity (assuming a material transformation) of series of subsets between the image corresponding to an initial and the one of the deformed studied state. The performance of this technique is closely related to local gradients of grey levels inside images [8]. These grey level values come from a speckle pattern at the surface which can be the natural texture of the specimen surface or an artificial pattern (deposited by spraying white and/or black paints).

Using DIC gives available results as shown in [6] but a bias exists [9]. Indeed the material transformation which is assumed homogeneous on a DIC subset cannot take into account the real discontinuous displacement field near the crack tip. For subsets crossing cracks, the measurement of displacement is disturbed by an unpredictable bias and the calculus of strains near these subsets is wrong. To avoid this problem, a manual inspection can be useful to detect the discontinuity path and to keep only the subsets on each side of the crack. This approach has been used a lot in fracture mechanics for straight cracks [7] and also with local analysis around the crack to determine opening displacements [10], [11]. The detection can be improved by using a mask given the location of cracks [9], [12] and the definition of subsets on the sides of cracks can be automated. Another solution

consists in changing the material transformation usually assuming homogeneous: a subset can be split in two parts with different kinematics [9], [13]. In this study, we propose a new DIC technique based on this last principle and especially developed for the study of the behaviour of flexible ceramics. The fracture characterization is here conducted through wedge splitting test (WST) which is well known for its ability to produce reliable data on stable crack propagation.

## 2. Materials and methods

### 2.1. Material

Magnesia-Spinel materials (MSp) have been investigated in this study. Thanks to a very high degree of refractoriness and to their resistance to basic environments, these refractory materials are typically used in steel making vessels or rotary cement kilns. Different MSp products exist, depending on the type of the spinel aggregates. Industrial bricks are usually obtained by uniaxial pressing of the raw materials and a sintering thermal cycle up to about 1600°C in order to obtain a rather dense refractory material (porosity about 15-16%). Due to thermal expansion mismatch between magnesia matrix ( $\sim 13.5 \cdot 10^{-6} \text{ }^\circ\text{C}^{-1}$ ) and spinel inclusions (less than  $10.3 \cdot 10^{-6} \text{ }^\circ\text{C}^{-1}$ ), microcracks are usually developed in the matrix around the spinel inclusions during the cooling stage of the process. Two types of industrial materials were studied here: MSp1 for which inclusions were aggregates of magnesium aluminate spinel ( $\text{MgAl}_2\text{O}_4$ ) and MSp2 for which inclusions were aggregates of iron aluminate spinel (Hercynite- $\text{FeAl}_2\text{O}_4$ ). Density and porosity of these composite materials are given in Table 1 as well as elastic properties measured by ultrasonic means. These measurements were evaluated on 5 samples of each material type. Since these two materials MSp1 and MSp2 don't contain the same kind of spinel exhibiting different coefficients of thermal expansion ( $\sim 7.6 \cdot 10^{-6} \text{ }^\circ\text{C}^{-1}$  for  $\text{MgAl}_2\text{O}_4$  in comparison to  $\sim 10.3 \cdot 10^{-6} \text{ }^\circ\text{C}^{-1}$  for  $\text{FeAl}_2\text{O}_4$ ), the microcrack network developed during cooling is not the same leading to some differences in elastic properties. From each type of material, two cubic-shaped specimens with cross-section of  $100 \times 100 \times 70 \text{ mm}^3$  were tested, although, in this paper only one will be presented since the results are quite similar. For image acquisition during mechanical loading and further numerical treatments, a great attention must be paid to sample surface preparation in order to avoid artefacts of correlation results between deformed and reference states. A black (or white) paint layer has been spread on specimen surface, and after drying, fine white (or black) droplets have been projected in order to constitute a speckle pattern useful for DIC. For this study, white droplets on a black surface were used.

**Table 1.** Properties of the studied MSp1 and MSp2 materials

	MSp1	MSp2
Density ( $\text{g}\cdot\text{cm}^{-3}$ )	2.94 (+/-0.01)	3.01 (+/- 0.02)
Porosity (%)	16.07 (+/- 0.50)	15.11 (+/- 0.29)
Young's modulus E (GPa)	31.43 (+/- 3.43)	39.26 (+/- 3.56)
Shear modulus G (GPa)	13.48 (+/- 1.79)	16.89 (+/- 1.61)
Poisson ratio $\nu$	0.17 (+/- 0.03)	0.16 (+/- 0.02)

### 2.2. Wedge Splitting Test

As other test methods like the notched beam test and the compact tension method, the wedge splitting test according to Tschegg [14], [15] allows to specify the mechanical fracturing properties of refractory materials under uniaxial load (mode I loading). This test, patented in 1986, is nowadays often applied on refractory materials to determine fracture mechanical properties (e.g. the specific fracture energy or the notch-tensile strength). The action of a wedge and the rather high rigidity of the equipment ensure a low energy accumulation in the specimen and the testing machine. Stable crack propagation can thus be easily achieved by displacement-controlled loading with a simple mechanical

or hydraulic testing device. The test configuration is represented in Figure 3. The specific sample geometry, with a groove in order to apply the splitting load and a starter notch, is manufactured by machining. The vertical action of a metallic wedge, placed on the upper part of the sample and in contact with movable rolls, entails horizontal forces thanks to load transmission pieces. Finally, the evolution of the horizontal force  $F_H$  versus the horizontal displacement  $\delta$  is registered.  $F_H$  is evaluated from the applied vertical load  $F_v$  taking into account the angle of the wedge and omitting the presence of friction.

From the curve horizontal load vs. horizontal displacements, elastic energy is estimated by assuming that an elastic linear unloading of the material reaches the initial state before mechanical sollicitation. It corresponds to the area enclosed in a triangle whose vertexes are the origin of the curve, the displacement and the applied load. The total energy is calculated by integrating the load-displacement curve.

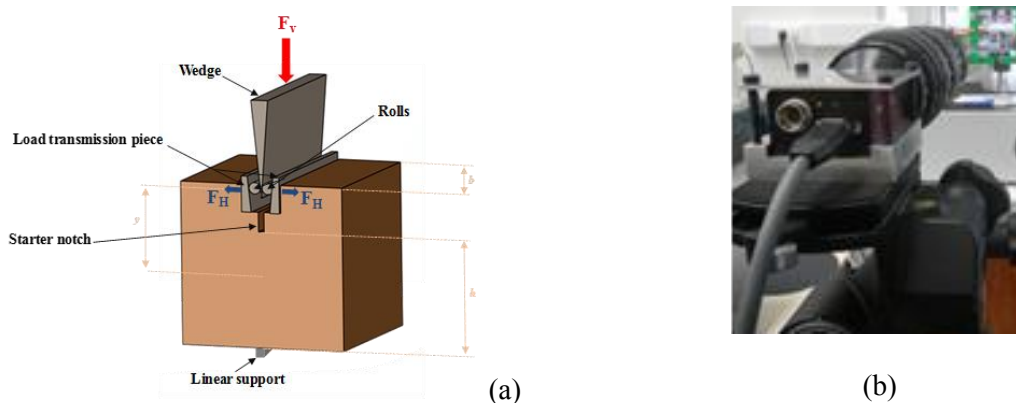


**Figure 3:** Principle of wedge splitting test with sample's geometry (a) and image acquisition setup (b)

### 2.3. 2P-DIC

#### 2.3.1. Principle

The new DIC technique, named two-parts DIC (2P-DIC) has especially been developed for the type of fracture observed in wedge splitting tests on refractory materials *i.e.* with a preferential direction of crack (here vertical) and a quasi-brittle mechanical behaviour. This technique is designed to detect the presence, the position and the opening of a crack. It uses the same principle of usual DIC for a

homogeneous material transformation  $\phi$  which is described by the vector  $\underline{q} = \left( u, v, \frac{\partial u}{\partial x}, \frac{\partial u}{\partial y}, \frac{\partial v}{\partial x}, \frac{\partial v}{\partial y} \right)$

gathering two translation parameters  $(u, v)$  and four components of local gradient [7]. The expression of correlation coefficient used to this study is given by the following formula:  $C(\underline{q}) = \sum_D c^2(\underline{q})$  with

$$c(\underline{q}) = \frac{\overline{f(\underline{x})}}{\overline{f(\underline{x})}} - \frac{\overline{g(\phi(\underline{X}))}}{\overline{g(\phi(\underline{X}))}} \quad (1)$$

where  $D$  is a subset,  $f$  and  $g$  represent the grey levels of pixels,  $\overline{f}$  and  $\overline{g}$  are their averages in  $D$  and  $\phi(D)$ ,  $\underline{X}$  and  $\underline{x}$  are the coordinates of grey levels for the reference and the deformed state respectively.

In the new proposed version of DIC, the subset  $D$  is divided vertically at the position  $XC$  in two parts  $D_1$  ( $x < XC$ ) and  $D_2$  ( $x > XC$ ) as shown Figure 4. The pixels at  $x=XC$  are not taken into account in the matching process.

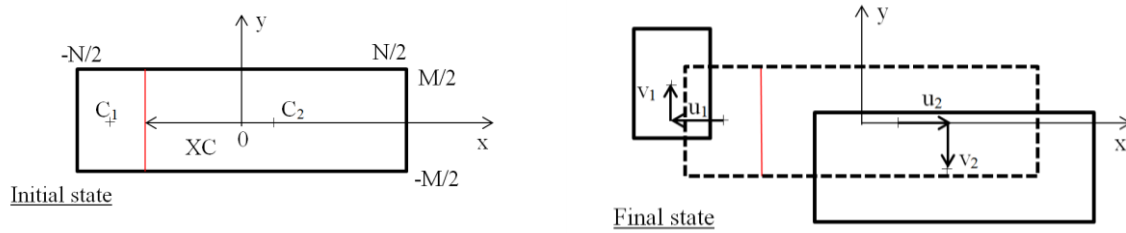


**Figure 4.** Principle of the 2P-DIC, decomposition of a subset.

For a given value of XC, the expression of correlation coefficient becomes:

$$C_{xc}(\underline{Q}) = \sum_{D_1} c^2(\underline{q}_1) + \sum_{D_2} c^2(\underline{q}_2) \quad (2)$$

With  $\underline{q}_i = \left( u_i, v_i, \frac{\partial u_i}{\partial x}, \frac{\partial u_i}{\partial y}, \frac{\partial v_i}{\partial x}, \frac{\partial v_i}{\partial y} \right)$  the vector of material transformation parameters in the part  $D_i$  ( $i=1,2$ ). The vector  $\underline{Q}$  represents all kinematic unknowns of  $D$  and is the gathering of two vectors  $\underline{q}_1$  and  $\underline{q}_2$ . The matching consists in searching the best values of XC and  $\underline{Q}$  which minimize  $C_{xc}(\underline{Q})$ . For each value of XC varying by one-pixel step from  $-N/4$  to  $N/4$ , a mean-square minimization process is used to achieve the best estimation of  $\underline{Q}$ . The values of XC smaller than  $-N/4$  and larger than  $N/4$  are not considered because they lead to a too small part  $D_i$  giving a displacement with an insufficient accuracy. We also have to note that considering the quasi-brittle behaviour of our material for this study we have neglected the local gradient parameters, and only the four components of rigid-body displacements are calculated. As crack propagation is almost vertical, we can here choose a rectangular subset with a height (M) smaller than the width (N) as shown Figure 4.

### 2.3.2. Crack detection

In previous studies [10], standard DIC was used to detect cracks according to the following method. Strain fields were calculated by finite differences [7] from displacement fields and a strain threshold  $\epsilon_s$  was defined to highlight the crack zone. Indeed crack presence corresponds to local higher strain values. This threshold  $\epsilon_s$  was set in order to extract the signal corresponding to reliable mechanical strains from fluctuations only due to DIC uncertainty. Thus cracks were detected with a rather large gauge length imposed by the initial choice of the subset size and of the grid step used to calculate strains by finite differences.

The proposed 2P-DIC gives a field of vectors  $\underline{Q}$  for each subset of the zone of interest of the sample and we can deduce a crack opening field from the difference of the displacements of each part of the subset  $D$ . To separate physical opening values to fluctuations due to 2P-DIC uncertainty, a thresholding is necessary. To have the same analysis way than the one for standard DIC, a pseudo strain field is calculated from the next expression  $\epsilon = (u_2 - u_1) / (XC_2 - XC_1)$  (for a vertical crack) and the threshold  $\epsilon_s$  is applied on this field. In this case, we have to note that the detection of horizontal crack position is determined with a resolution equal to one pixel in x direction.

### 3. Results

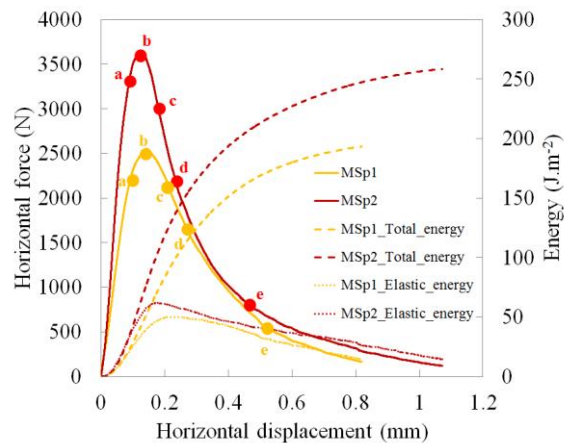
#### 3.1. Load-displacement curves obtained by WST

Figure 5 represents the typical horizontal load-displacement curves of the two studied materials obtained by WST. The mechanical behaviour is characterized by three stages: (1) the first stage corresponds to linear elastic behaviour, (2) the beginning of non-linearity is related to the occurrence of very first microcracks within the microstructure close to the notch, (3) the maximum of the curve is linked to the macro-crack onset (the following part of the curve representing the macrocrack propagation). The horizontal load-displacement curve of MSp1 exhibits a lower maximum load in comparison to MSp2, thus the replacement of  $MgAl_2O_4$  aggregates by hercynite aggregates seems here to increase the fracture energy which moves from  $172 \text{ J.m}^{-2}$  for MSp1 to  $227 \text{ J.m}^{-2}$  for MSp2.

In order to visualise the microcrack onset (stage 2) and macrocrack propagation (stage 3), different states, from (a) to (e) have been chosen (Figure 5) to compare results obtained by 2P-DIC and standard DIC. Taking into account fluctuations in  $\epsilon$  only due uncertainty for each treatment, related to subset size and step between subsequent subsets used to calculate  $\epsilon$ , the thresholds  $\epsilon_s$  have been adjusted to 0.002 for DIC and to 0.003 for 2P-DIC.

#### 3.2. Visualisation of microcracks onset and macrocrack propagation in the case of MSp1

From the same images acquired during the same wedge splitting test on MSp1 material, Figures 6 and 7 present the results of standard DIC and 2P-DIC respectively for states (a) to (e) previously indicated in Figure 5. At first glance, one could observe that both approaches lead to a rather unique crack for states (a) to (c) and then, that large crack branching can be detected in states (d) and (e). It seems here that DIC and 2P-DIC reveal the same cracks but with a much better spatial resolution for the latter. Looking more carefully to the different thumbnails on Figure 7, particularly usefully in the case of 2P-DIC treatment for which each individual crack thickness is typically drawn at least with one pixel, one could notice that even in the early stages (states (a) and (b)), not only one single microcrack is observed (in contrast to standard DIC for these same first states). In same trend, one could also observe that, for state (d), 2P-DIC is able to reveal crack branching in the upper part of the global picture which is not detected by standard DIC. At this state, in some zones, the thickness of the cracks is larger than one pixel and one can observe their opening.



**Figure 5.** Horizontal load and energies versus horizontal load displacement for MSp1 and MSp2

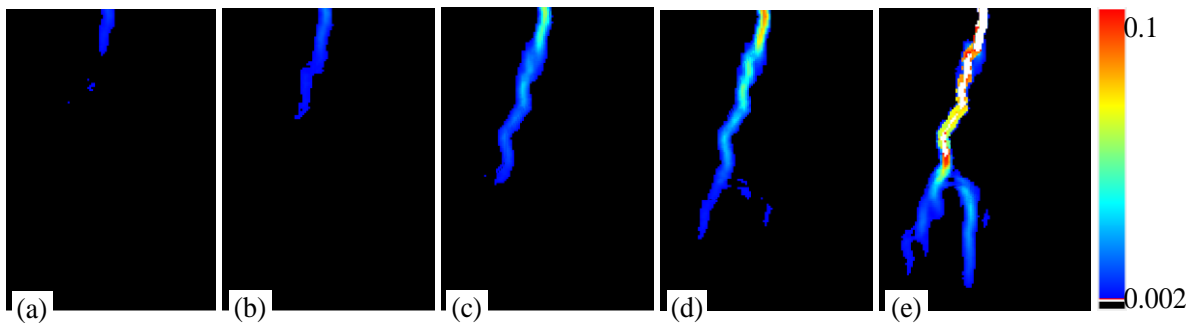


**Figure 6.** Standard DIC horizontal strain field with  $\epsilon_s=0.002$ , subset size 32x32 pixels, subset shift 8 pixels, strain gauge length 32 pixels

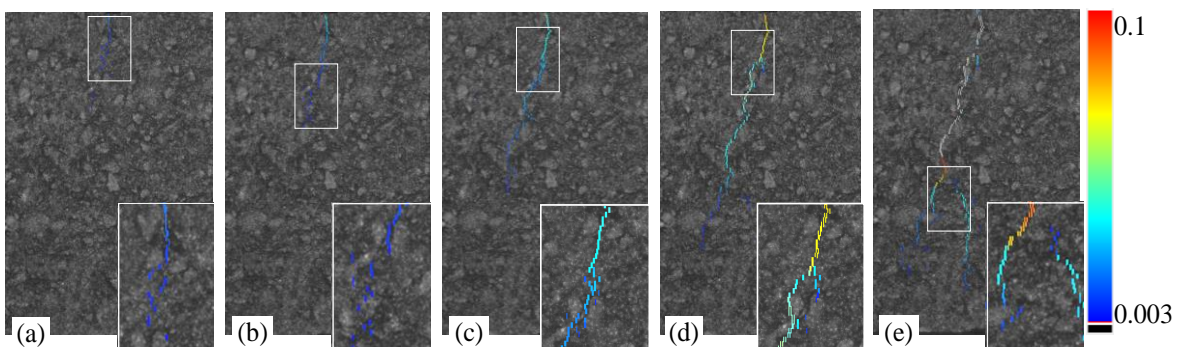


**Figure 7.** 2P-DIC crack opening by plotting  $\epsilon$  for  $\epsilon_s=0.003$ , subset size 64x8 pixels.

### 3.3. Visualisation of microcracks onset and macrocrack propagation in the case of MSp2

In a similar way to previous results, from the same images acquired during the same wedge splitting test on MSp2 material, Figures 8 and 9 present the results of standard DIC and 2P-DIC respectively for states (a) to (e) previously indicated in Figure 5. Same general comments can be done here: DIC and 2P-DIC detects the same global crack path but with a much better spatial resolution for 2P-DIC. Nevertheless, one could notice that the crack branching phenomenon takes place earlier (state (c) here in comparison to state (d) for MSp1) and is much more developed in further states (states (d) and (e)). This important microstructural feature leads to the larger specific fracture energy measured on this second material. Again, looking more carefully to the different thumbnails on Figure 9, it seems that even in the very early stages (stage (a) and (b)), the different very small microcracks are possibly more dispersed (in comparison to same stages on material MSp1), which leads further to more numerous branches when actual crack branching phenomenon will take place (especially in stage (d)). This very interesting point has to be related to voluntary introduced network of microcracks in the initial microstructure of these materials.

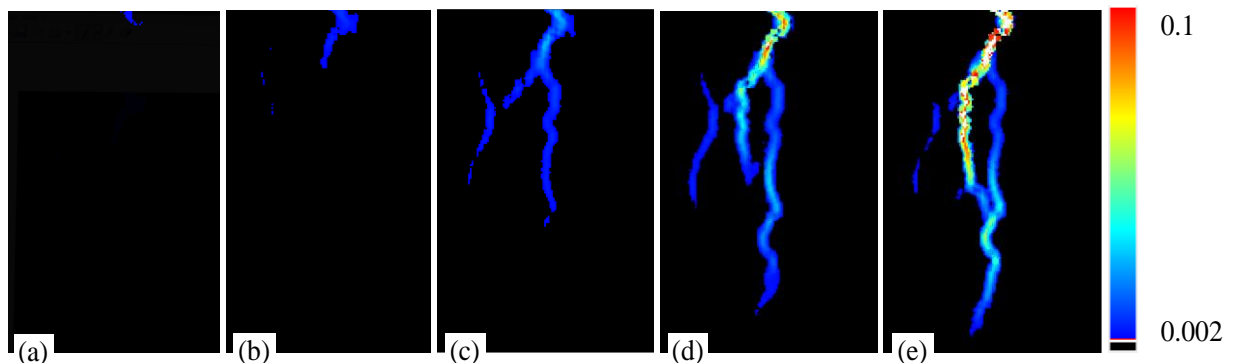


**Figure 8.** Standard DIC horizontal strain field with  $\varepsilon_s=0.002$ , subset size 32x32 pixels, subset shift 8 pixels, strain gauge length 32 pixels

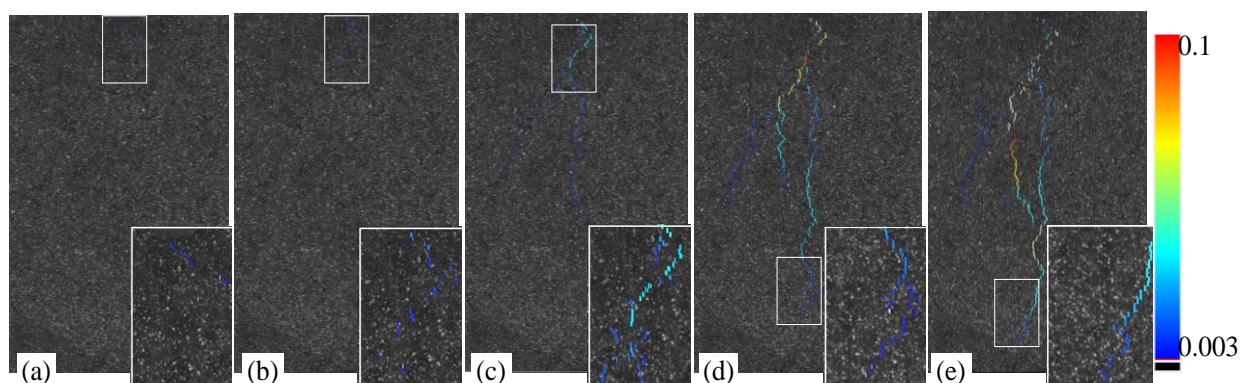


**Figure 9.** 2P-DIC crack opening by plotting  $\varepsilon$  for  $\varepsilon_s=0.003$ , subset size 64x8 pixels.

#### 4. Conclusion

Thermal shock resistance of refractories is known to be closely related to the crack growth behaviour. This property can be optimized in industrial materials by a voluntary introduced micro-cracked network within the initial microstructure moving the mechanical stress-strain law from a elastic behaviour to a nonlinear one, thus enhancing surface fracture energy as well as strain to rupture. The recent development of optical methods for kinematic field measurement and associated dedicated numerical treatments is a promising route for improvement in the understanding of fracture mechanisms in these heterogeneous materials. Recent refinement of Digital Image Correlation technique with an adapted 2P-DIC treatment applied in this study on two magnesia-spinel materials illustrates the advantage which can be obtained in the case of wedge splitting test. The obtained results highlighted in particular the efficiency of this new technique to early detect crack path with an optimal spatial resolution. For the studied materials, it allows to underline the occurrence of the crack branching phenomenon, induced by the thermal expansion mismatch between the different phases with a significant differentiation between materials containing  $MgAl_2O_4$  aggregates or hercynite aggregates. Besides, this optimized 2P-DIC method that allows to automatically determine the crack path with an interesting spatial accuracy, opens new way to correlated actual crack(s) length with the so-called specific fracture energy which plays a key role in the thermal shock resistance of refractories.

#### Acknowledgements

This work is a part of a global research program engaged through collaboration within the F.I.R.E network. The authors are thankful to RHI AG for providing the materials.

## References

- [1] G. A. Gogotsi, Y. L. Groushevsky, K. K. Strelov, The significance of non-elastic deformation in the fracture of heterogeneous ceramic materials, *Ceramurg. Int.*, **4**, 1978, 113-118.
- [2] H. Harmuth, E. K. Tschegg, A fracture mechanics approach for the development of refractory materials with reduced brittleness, *Fatigue Fract. Eng. Mater. Struct.*, **20**, 1997, 1585-1603.
- [3] M. Huger, N. Tessier-Doyen, T. Chotard, C. Gault, Microstructural effects associated to CTE mismatch for enhancing the thermal shock resistance of refractories: Investigation by high temperature ultrasounds, *CFI Ceram. Forum Int.* **84**, 2007, E93-E102.
- [4] R. C. Bradt, Problems and possibilities with cracks in ceramics, *Science of Ceramics*, 1981, 349-360.
- [5] H. A. Bruck, S. R. McNeill, M. A. Sutton and W. H. Peters, Digital image correlation using newton-raphson method of partial differential correction, *Experimental Mechanics*, vol. 29, no. 3, pp. 261-267, 1989
- [6] S. Choi and S. P. Shah, Measurement of Deformations on Concrete Subjected to Compression Using Image Correlation, *Experimental Mechanics*, vol. 37, no. 3, pp. 307-313, 1997.
- [7] Y. Barranger, P. Doumalin, J. Dupré and A. Germaneau, Strain Measurement by Digital Image Correlation: Influence of Two Types of Speckle Patterns Made from Rigid or Deformable Marks, *Strain*, 2012.
- [8] M. Bornert, F. Brémand, P. Doumalin, J.-C. Dupré, M. Fazzini, M. Grédiac, F. Hild, S. Mistou, J. Molimard, J.-J. Orteu, L. Robert, Y. Surrel, P. Vacher and B. Wattrisse, Assessment of digital image correlation measurement errors: Methodology and results, *Experimental Mechanics*, vol. 49, no. 3, pp. 353-370, 2009.
- [9] J. C. Dupré, P. Doumalin, H. A. Hussein, A. Germaneau and F. Brémand, Displacement Discontinuity or Complex Shape of Sample: Assessment of Accuracy and Adaptation of Local DIC Approach, *Strain*, Article first published online: 29 JUL 2015, DOI: 10.1111/str.12150.
- [10] Y. Belrhiti, O. Pop, A. Germaneau, P. Doumalin, J.C. Dupré, H. Harmuth, M. Huger, T. Chotard; Investigation of the impact of micro-cracks on fracture behavior of magnesia products using wedge splitting test and digital image correlation , *Journal of European Ceramic Society*, **35**(2), pp823-829, 2015
- [11] J. Réthoré and R. Estevez, Identification of a cohesive zone model from digital images at the micron-scale, *Journal of the Mechanics and Physics of Solids*, vol. 61, p. 1407–1420, 2013
- [12] Q. Zhang and J. Zhao, Determination of mechanical properties and full-field strain measurements of rock material under dynamic loads, *International Journal of Rock Mechanics & Mining Sciences*, vol. 60, p. 423–439, 2013
- [13] L. Nunes and J. Reis, Estimation of crack-tip-opening displacement and crack extension of glass fiber reinforced polymer mortars using digital image correlation method, *Materials and Design*, vol. 33, p. 248–253, 2012
- [14] E.K. Tschegg, Equipment and appropriate specimen shapes for tests to measure fracture values, 31.1.1986, AT no. 390328, Austrian Patent Office, Austria (Prüfeinrichtung zur Ermittlung von bruchmechanischen Kennwerten sowie hierfür geeignete Prüfkörper, 31.1.1986, Patentschrift Nr. 390328).
- [15] E.K. Tschegg, New equipment for fracture tests on concrete, *Mater. Test. (Mater)*, **33**, 1991, 338-342.